INTERNATIONAL JOURNAL FOR NUMERICAL METHODS IN ENGINEERING, VOL. 30, 1577–1593 (1990)

FINITE ELEMENT ANALYSIS OF SHEET METAL FORMING PROBLEMS USING A SELECTIVE VISCOUS BENDING/MEMBRANE FORMULATION

E. OÑATE AND C. AGELET DE SARACIBAR

International Center for Numerical Methods in Engineering, E.T.S. Ingenieros de Caminos, Universidad Politécnica de Cataluña 08034 Barcelona, Spain

SUMMARY

In this paper the possibilities of the viscous voided shell approach for deriving bending/membrane finite elements for sheet metal forming problems are presented. These elements can be selectively used for membrane or full bending analysis of some parts of the sheet according to the nature of the deformation. Numerical aspects of this approach are discussed and some examples of application are also given.

INTRODUCTION

Over the years flow formulation has proved to be a simple and effective procedure for finite element analysis of metal forming problems.[1–6] The inclusion of void degradation effects in the viscoplastic flow model introduces compressibility and the resulting formulation is analogous to standard non-linear elasticity theory.[7] This analogy provides a basis for deriving a 'viscous shell' formulation for analysis of sheet metal forming problems in a simple and straightforward manner.[5,7]

The objective of this paper is to show the possibilities of the viscous shell approach for deriving membrane and bending viscous finite elements. These elements can be used in different parts of the sheet in a selective hierarchical manner according to the specific features of the sheet deformation pattern.

The content of the paper is the following. In the first part a summary of the basic concepts of the 'viscous voided' flow approach is given. Then the basis of the finite element viscous shell formulation for sheet metal forming problems is presented and some numerical aspects of the solution algorithm are discussed. In the next section details of the full axisymmetric viscous shell formulation are given and an algorithm for the selective choice of membrane or bending elements in different parts of the sheet is presented. Finally, some examples of applications of the proposed algorithm are presented.

BASIC CONCEPTS

The basis of the 'flow approach' is the assumption that the deforming material behaves like an equivalent fluid with strain rates $\dot{\varepsilon}_{ij}$ and velocities u_i related by

$$\dot{\varepsilon}_{ij} = \frac{1}{2}\left(\frac{\partial u_i}{\partial x_j} + \frac{\partial u_j}{\partial x_i}\right) \quad \text{or} \quad \dot{\boldsymbol{\varepsilon}} = \mathbf{L}\mathbf{u} \tag{1}$$

0029–5981/90/161577–17$08.50
© 1990 by John Wiley & Sons, Ltd.
Received September 1989

and the stresses satisfy the standard equilibrium conditions[8]

$$\begin{aligned} \mathbf{L}^{\mathrm{T}}\boldsymbol{\sigma} + \mathbf{b} = 0 \quad &\text{in the volume } V \\ \mathbf{M}^{\mathrm{T}}\boldsymbol{\sigma} - \mathbf{t} = 0 \quad &\text{in the boundary } \Gamma \end{aligned} \tag{2}$$

where $\mathbf{b}$ and $\mathbf{t}$ are body force and surface loads, respectively, and $\mathbf{M}$ is a matrix containing the components of the unit normal to the boundary Γ.

We consider here the flow of a pure plastic/viscoplastic metal in which elastic effects are neglected. Further, the constitutive model used is based on Gurson's theory for void containing metals.[9] Under these assumptions, and using standard plasticity theory, the constitutive equation relating strain rates and stresses can be written in the following rate form:[7,10-12]

$$\dot{\varepsilon}_{ij} = \dot{\varepsilon}_{ij}^{\mathrm{NL}} = \frac{1}{2\bar{G}}\left[\sigma_{ij} - \frac{\bar{\nu}}{1+\bar{\nu}}\sigma_{kk}\delta_{ij}\right] \tag{3}$$

where $\dot{\varepsilon}_{ij}$ and $\dot{\varepsilon}_{ij}^{\mathrm{NL}}$ account for the total and non-linear plastic/viscoplastic strain rate tensors, respectively.

Note the analogy of (1), (2) and (3) with the strain–displacement, equilibrium and stress–strain relationships of elasticity theory.[8] The problem can then be stated as one of standard elasticity with displacements and strains playing the role of velocities and strain rates, respectively, and $\bar{G}$ and $\bar{\nu}$ being the equivalent 'elastic shear modulus' and Poisson's ratio, respectively. The values of the equivalent elastic material parameters $\bar{G}$ and $\bar{\nu}$ can be obtained as[7,10-12]

Viscoplastic flow: $(\bar{\sigma}_{\mathrm{M}} = \sigma_{\mathrm{M}} + k\dot{\bar{e}}_{\mathrm{M}}^{m})$

$$\begin{aligned} \bar{G} &= \frac{\sigma_{\mathrm{M}} w}{3\dot{\bar{e}}_{\mathrm{M}}} + \frac{1}{3} k w \dot{\bar{e}}_{\mathrm{M}}^{m-1} \\ \bar{\nu} &= \frac{1 - BC^2}{2 + BC^2} \end{aligned} \tag{4}$$

with

$$\begin{aligned} B &= \frac{f\sinh(A)}{2A}, \quad A = \frac{\sigma_{kk}}{2\sigma_{\mathrm{M}}} \\ k &= \left(\frac{1}{\gamma}\right)^{m}, \quad m = \frac{1}{n}, \quad C = \left(1 + \frac{k}{\sigma_{\mathrm{M}}}\dot{\bar{e}}_{\mathrm{M}}^{m}\right) \\ \dot{\bar{e}}_{\mathrm{M}} &= \left(\frac{2}{3}\dot{e}_{ij}^{\mathrm{vp}}\dot{e}_{ij}^{\mathrm{vp}} w\right)^{1/2} \end{aligned} \tag{5}$$

where σ_{M} is the tensile yield limit of the matrix material, f is the void volume fraction, γ is the fluidity parameter, n is the exponent of the yield function in the viscoplastic law, $\dot{e}_{ij}^{\mathrm{vp}}$ is the deviatoric viscoplastic strain rate tensor and $w = 1 - 2f\cosh(A) + f^2$.[7,10-12]

Plastic flow: $(\bar{\sigma}_{\mathrm{M}} = \sigma_{\mathrm{M}})$

The equations for plastic flow are simply obtained by making $k = 0$ in (4) and (5). This yields

$$\begin{aligned} \bar{G} &= \frac{\sigma_{\mathrm{M}} w}{3\dot{\bar{e}}_{\mathrm{M}}} \\ \bar{\nu} &= \frac{1 - B}{2 + B} \end{aligned} \tag{6}$$

Equations (1) and (6) are completed with the adecuate evolution law for the void volume fraction which can be taken as

$$\dot{f} = \dot{f}_g + \dot{f}_n + \dot{f}_c \tag{7}$$

where subscripts g, n and c stand for growth, nucleation and coalescence of voids. For details of the different terms of (7) see References 7 and 13.

Note that the inclusion of the effect of voids results in a 'compressible' flow with $\bar{\nu} \neq \frac{1}{2}$. For non-voided metals $f = 0$ and (4) and (6) are

Viscoplastic flow:

$$\bar{G} = \frac{\sigma_M + \left(\frac{\dot{\bar{\varepsilon}}}{\gamma}\right)^m}{3\dot{\bar{\varepsilon}}}, \quad \bar{\nu} = \frac{1}{2} \tag{8}$$

Plastic flow:

$$\bar{G} = \frac{\sigma_M}{3\dot{\bar{\varepsilon}}}, \quad \bar{\nu} = \frac{1}{2} \tag{9}$$

with now

$$\dot{\bar{\varepsilon}} = \dot{\bar{e}} = \left(\frac{2}{3}\dot{\varepsilon}_{ij}^{vp}\dot{\varepsilon}_{ij}^{vp}\right)^{1/2}$$

Thus the 'incompressible' form of the deformation is recovered and the expression of the equivalent shear modulus coincides with that of the non-Newtonian viscosity of the standard flow problem.[2]

APPLICATION TO THIN SHEET METAL FORMING PROBLEMS

The theory presented in the preceding section allows the analysis of plastic/viscoplastic deformation of thin sheets of metal by making direct use of classical small displacement elastic shell theory. The solution scheme is thus as follows.

1. Identify an elastic shell formulation. If standard finite element techniques are used[8] the discrete system of equations can be written in the form

$$\mathbf{K}(G, \nu)\mathbf{a} = \mathbf{f} \tag{10}$$

   where $\mathbf{K}$ is the secant stiffness matrix of the sheet and $\mathbf{a}$ and $\mathbf{f}$ are the displacement and nodal force vectors, respectively. The equivalent 'viscous shell' theory is formulated by simply identifying displacements and strains with velocities and strain rates, respectively, and substituting the shear modulus and Poisson's ratio by the non-linear parameters $\bar{G}$ and $\bar{\nu}$ of the preceding section.
2. Solve iteratively the resulting non-linear system (10) for the velocity field. Some numerical aspects of this solution are discussed in the next section.
3. Restart the process with new updated values of the sheet geometry, boundary conditions and void volume fraction.[7]

The above algorithm allows one to include other important effects like strain hardening and contact frictional conditions in a simple manner.[7,12,14]

SOME NUMERICAL ASPECTS OF THE NON-LINEAR SOLUTION

The resulting non-linear equilibrium system (10) can be written in the form

$$\mathbf{r}(\mathbf{a}, \mathbf{x}, t) = \mathbf{p}(\mathbf{a}, \mathbf{x}) - \mathbf{f}(t, \mathbf{x}) = \mathbf{0} \tag{11}$$

where $\mathbf{r}$ is the residual force vector, $\mathbf{f}$ the vector of external nodal forces and $\mathbf{p}$ the internal force vector given by

$$\mathbf{p}(\mathbf{a}, \mathbf{x}) = \mathbf{K}(\mathbf{a}, \mathbf{x})\mathbf{a} \tag{12}$$

In (11) and (12) $\mathbf{a}$ and $\mathbf{x}$ are the nodal velocity and spatial co-ordinate fields, respectively, and t is the time. These variables are not independent and they can be related by the following time integration scheme:

$$^{t+\Delta t}\mathbf{x} = {}^{t}\mathbf{x} + {}^{t}\mathbf{a}(1-\theta)\Delta t + {}^{t+\Delta t}\mathbf{a}\theta\Delta t \tag{13}$$

where $0 \leqslant \theta \leqslant 1$.

For $\theta = 0$ the integration scheme (13) is explicit and the equilibrium equation (11) can be written and solved at time t for the nodal velocities ${}^{t}\mathbf{a}$ with known values of the co-ordinates ${}^{t}\mathbf{x}$. On the other hand, $\theta \neq 0$ yields an implicit scheme and (11) is written at $t + \Delta t$ with both ${}^{t+\Delta t}\mathbf{a}$ and ${}^{t+\Delta t}\mathbf{x}$ as unknowns, related by (13).

Table I shows the solution algorithm using a predictor–corrector incremental iterative scheme.

Table I. Predictor–corrector algorithm

1. *Initialization*

$$t = 0, \quad {}^{0}\mathbf{a} = 0, \quad {}^{0}\mathbf{x} = \mathbf{x}$$

2. *Predictor*

$$k = 0$$

$$^{t+\Delta t}\mathbf{a}^{0} = {}^{t}\mathbf{a}, \quad {}^{t+\Delta t}\mathbf{x}^{0} = {}^{t}\mathbf{x} + {}^{t}\mathbf{a}\Delta t$$

3. *Corrector*

3.1 Compute residual forces

$$^{t+\Delta t}\mathbf{r}^{k} = {}^{t+\Delta t}\mathbf{p}^{k} - {}^{t+\Delta t}\mathbf{f}^{k}$$

3.2 Compute error norm

$$E = \frac{\| {}^{t+\Delta t}\mathbf{r}^{k} \|}{\| {}^{t+\Delta t}\mathbf{f}^{k} \|}$$

3.3 Check convergence

if (E. LT. TOL) GO TO 4

3.4 Form iteration matrix ${}^{t+\Delta t}\mathbf{H}^{k}$

3.5 Solve the system of equations

$$\Delta\mathbf{a}^{k} = -({}^{t+\Delta t}\mathbf{H}^{k})^{-1}({}^{t+\Delta t}\mathbf{r}^{k})$$

3.6 Update variables

$$^{t+\Delta t}\mathbf{a}^{k+1} = {}^{t+\Delta t}\mathbf{a}^{k} + \Delta\mathbf{a}^{k}$$

$$^{t+\Delta t}\mathbf{x}^{k+1} = {}^{t}\mathbf{x} + {}^{t}\mathbf{a}(1-\theta)\Delta t + {}^{t+\Delta t}\mathbf{a}^{k+1}\theta\Delta t$$

3.7 $k = k + 1$

GO TO 3.1

4. *Output results*

There are different possibilities for choosing matrix **H** for the solution of the equation system (see step 3.5 in Table I). A simple option is to make **H** equal to the secant stiffness matrix **K** of (10). This, together with an explicit scheme ($\theta = 0$), is identical for using a direct iteration scheme which has proved to yield convergence in a reasonable number of iterations in many practical cases.[2,7]

A second alternative is to make $\mathbf{H} = \mathbf{K}_T$, where $\mathbf{K}_T$ is the standard tangent matrix defined by

$$\mathbf{K}_T = \frac{\mathrm{Dr}}{\mathrm{Da}} = \frac{\mathrm{Dp}}{\mathrm{Da}} - \frac{\mathrm{Df}}{\mathrm{Da}} \tag{14}$$

The exact computation of $\mathbf{K}_T$ for the full viscous voided formulation is complicated and the resulting expression is non-symmetric.[11] Some of these difficulties have been overcome by the authors by using a simpler approximation for $\mathbf{K}_T = \hat{\mathbf{K}}_T$ given by

$$\hat{\mathbf{K}}_T = \frac{\partial \mathbf{K}}{\partial \mathbf{a}}\mathbf{a} + \mathbf{K} = \mathbf{H} \tag{15}$$

Numerical experiments have shown that the use of (15) for **H** yields convergence of the algorithm of Table I in approximately one half the number of iterations for the direct iteration scheme.

AXISYMMETRIC VISCOUS SHELL FORMULATION

The basis of the success of the viscous shell approach therefore lies in the efficiency of the analogous elastic shell formulation. We will present here a formulation based on Reissner–Mindlin axisymmetric shell theory.[1,2] Figure 1 shows a typical geometry of an axisymmetric sheet discretized in two node troncoconical elements.

The velocity field, after discretization, can be expressed as

$$\mathbf{u} = \begin{Bmatrix} u \\ w \\ \theta \end{Bmatrix} = \sum_{i=1}^{2} \mathbf{N}_i \mathbf{a}_i \tag{16}$$

with

$$\mathbf{N}_i = N_i \mathbf{I}_3 \quad \text{and} \quad \mathbf{a}_i = \begin{Bmatrix} u_i \\ w_i \\ \theta_i \end{Bmatrix} \tag{17}$$

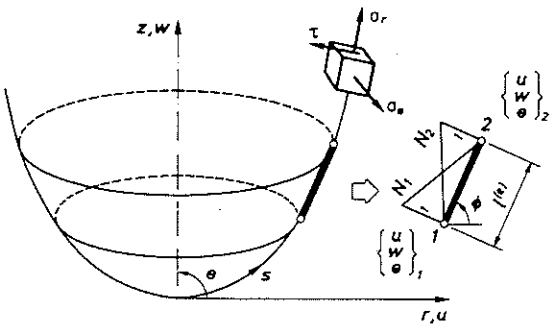

Figure 1. Axisymmetric shell. Discretization in axisymmetric linear elements

with u_i, w_i and θ_i being the two global velocities and the angular velocity of node i, respectively, and N_i the linear shape function of node i (Figure 1).

The generalized strain rate and resultant stress vectors in each element can be expressed as

$$\dot{\boldsymbol{\varepsilon}} = \begin{Bmatrix} \dot{\boldsymbol{\varepsilon}}_m \\ \dot{\boldsymbol{\varepsilon}}_b \\ \dot{\boldsymbol{\varepsilon}}_s \end{Bmatrix} = \sum_{i=1}^{2} \mathbf{B}_i \mathbf{a}_i \tag{18}$$

$$\boldsymbol{\sigma} = \begin{Bmatrix} \boldsymbol{\sigma}_m \\ \boldsymbol{\sigma}_b \\ \boldsymbol{\sigma}_s \end{Bmatrix} = \mathbf{D}\dot{\boldsymbol{\varepsilon}} = \mathbf{D} \sum_{i=1}^{2} \mathbf{B}_i \mathbf{a}_i \tag{19}$$

where subscripts m, b and s denote membrane, bending and shear terms respectively. The expressions for the above vectors and matrices are shown in Table II.

After adequate substitution of (16)–(19) in the rate of virtual work the following system of equations can be obtained:[7]

$$\mathbf{r} = \mathbf{K}(\mathbf{a})\mathbf{a} - \mathbf{f} = 0 \tag{20}$$

The element contributions to the stiffness matrix $\mathbf{K}$ and the nodal forces vector $\mathbf{f}$ are

$$\mathbf{K}_{ij}^{(e)} = 2\pi \int_{l^{(e)}} \mathbf{B}_i^T \mathbf{D} \mathbf{B}_j r \, ds \tag{21}$$

$$\mathbf{f}_i^{(e)} = 2\pi \int_{l^{(e)}} \mathbf{N}_i \mathbf{t} r \, ds + 2\pi r_i \mathbf{p}_i \tag{22}$$

where $l^{(e)}$ is the element length, r the radial distance and $\mathbf{t}$ and $\mathbf{p}_i$ surface and point load vectors, respectively.

Note the non-linearity of (20) due to the stress and strain dependence of parameters $\bar{G}$ and $\bar{\nu}$ (see (4)–(9)). Equation (20) can be solved using the incremental-iterative predictor–corrector algorithm of Table I.

It has been shown by Oñate and co-workers[5,7] that for a successful use of this formulation for thin sheet analysis the element stiffness matrix of (37) must be numerically computed using a single Gaussian integration point. In practice this simply implies obtaining $\mathbf{K}_{ij}^{(e)}$ explicitly as

$$\mathbf{K}_{ij}^{(e)} = 2\pi \bar{\mathbf{B}}_i^T \bar{\mathbf{D}} \bar{\mathbf{B}}_j \bar{r} l^{(e)} \tag{23}$$

where $\bar{(\cdot)}$ denotes values at the element midpoint. The expression of $\bar{\mathbf{B}}_i$ is readily obtained by substituting the terms N_i and $\partial N_i/\partial s$ in Table II by $\frac{1}{2}$ and $(-1)^i/l^{(e)}$, respectively.

SELECTIVE BENDING/MEMBRANE FORMULATION

Recently Oñate and Agelet de Saracibar[12,15,16] have shown the possibilities of the viscous shell formulation for deriving a selective bending/membrane approach. In this, bending and membrane elements are used in a selective manner in accordance with the specific features of the sheet deformation pattern at each deforming step, i.e. membrane elements are used in zones where the shell is basically under tension conditions, whereas in zones where bending effects are predominant (i.e. sharp corners) a bending formulation is chosen. To explain this procedure we will consider a sheet discretized in flat viscous shell elements. An example of this is the troncoconical elements for axisymmetric shell analysis studied in the preceding section or any of the flat

Table II. Axisymmetric viscous shell: Generalized strain rate–velocity and constitutive relationships

$$\dot{\boldsymbol{\varepsilon}} = \begin{Bmatrix} \dot{\boldsymbol{\varepsilon}}_m \\ \dot{\boldsymbol{\varepsilon}}_b \\ \dot{\boldsymbol{\varepsilon}}_s \end{Bmatrix} = \begin{Bmatrix} \dot{\varepsilon}_r \\ \dot{\varepsilon}_\theta \\ \hline \dot{\chi}_r \\ \dot{\chi}_\theta \\ \hline \dot{\gamma} \end{Bmatrix} = \begin{Bmatrix} C\dfrac{\partial u}{\partial s} + S\dfrac{\partial w}{\partial s} \\ \dfrac{u}{r} \\ \hline \\ -\dfrac{\partial \theta}{\partial s} \\ -\dfrac{\theta \cos\phi}{r} \\ \hline \\ -S\dfrac{\partial u}{\partial s} + C\dfrac{\partial w}{\partial s} - \theta \end{Bmatrix} = \sum_{i=1}^{2} \mathbf{B}_i \mathbf{a}_i$$

$$\mathbf{B}_i = \begin{Bmatrix} \mathbf{B}_{m_i} \\ \mathbf{B}_{b_i} \\ \mathbf{B}_{s_i} \end{Bmatrix} = \begin{bmatrix} C\dfrac{\partial N_i}{\partial s} & S\dfrac{\partial N_i}{\partial s} & 0 \\ \dfrac{N_i}{r} & 0 & 0 \\ \hline 0 & 0 & -\dfrac{\partial N_i}{\partial s} \\ 0 & 0 & -\dfrac{N_i C}{r} \\ \hline -S\dfrac{\partial N_i}{\partial s} & C\dfrac{\partial N_i}{\partial s} & -N_i \end{bmatrix}$$

$$S = \sin\phi; \quad C = \cos\phi$$

$$\boldsymbol{\sigma} = [N_r, N_\theta, M_r, M_\theta, Q]^{\mathrm{T}} = \mathbf{D}\dot{\boldsymbol{\varepsilon}} = \mathbf{D} \sum_{i=1}^{2} \mathbf{B}_i \mathbf{a}_i$$

$$\mathbf{D} = \begin{bmatrix} \mathbf{D}_m & \mathbf{D}_{mb} & 0 \\ \mathbf{D}_{mb} & \mathbf{D}_b & 0 \\ 0 & 0 & D_s \end{bmatrix} = \int_{-t/2}^{t/2} \begin{bmatrix} \hat{\mathbf{D}}_m & z'\hat{\mathbf{D}}_m & \mathbf{0} \\ z'\hat{\mathbf{D}}_m & (z')^2\hat{\mathbf{D}}_m & \mathbf{0} \\ 0 & 0 & D_c \end{bmatrix} dz'$$

$$\hat{\mathbf{D}}_m = \frac{2\bar{G}}{1-\bar{\nu}} \begin{bmatrix} 1 & \bar{\nu} \\ \bar{\nu} & 1 \end{bmatrix}; \quad D_c = \bar{G}$$

elements traditionally used for 3D shell analysis.[8] For any of these elements the stiffness matrix $\mathbf{K}$ of (21) can be written in the form

$$\mathbf{K}^{(e)} = \mathbf{K}_{m}^{(e)} + \mathbf{K}_{b}^{(e)} + \mathbf{K}_{mb}^{(e)} + \mathbf{K}_{s}^{(e)} \tag{24}$$

where subscripts m, b, mb and s denote membrane, bending, membrane–bending coupling and shear contributions to the total stiffness matrix of the element. An example of the form of the above matrices for the simple two node axisymmetric viscous element is the following:

$$\mathbf{K}_{m_{ij}}^{(e)} = 2\pi\bar{r}l^{(e)}\bar{\mathbf{B}}_{m_i}^{T}\bar{\mathbf{D}}_{m}\bar{\mathbf{B}}_{m_j} \tag{25}$$

$$\mathbf{K}_{b_{ij}}^{(e)} = 2\pi\bar{r}l^{(e)}\bar{\mathbf{B}}_{b_i}^{T}\bar{\mathbf{D}}_{b}\bar{\mathbf{B}}_{b_j} \tag{26}$$

$$\mathbf{K}_{mb_{ij}}^{(e)} = 2\pi\bar{r}l^{(e)}[\bar{\mathbf{B}}_{m_i}^{T}\bar{\mathbf{D}}_{mb}\bar{\mathbf{B}}_{b_j} + \bar{\mathbf{B}}_{b_i}^{T}\bar{\mathbf{D}}_{mb}\bar{\mathbf{B}}_{m_j}] \tag{27}$$

$$\mathbf{K}_{s_{ij}}^{(e)} = 2\pi\bar{r}l^{(e)}\bar{\mathbf{B}}_{s_i}^{T}\bar{\mathbf{D}}_{s}\bar{\mathbf{B}}_{s_j} \tag{28}$$

where the different $\mathbf{B}$ and $\mathbf{D}$ matrices can be obtained from Table II.

Expression (24) allows one to compute the energy rates for the element at each deformation stage once the velocity field has been found from (20). Thus we can define for each element

$$\dot{U}^{(e)} = \tfrac{1}{2}[\mathbf{a}^{(e)}]^{T}\mathbf{K}^{(e)}\mathbf{a}^{(e)} \tag{29}$$

$$\dot{U}_{m}^{(e)} = \tfrac{1}{2}[\mathbf{a}^{(e)}]^{T}\mathbf{K}_{m}^{(e)}\mathbf{a}^{(e)} \tag{30}$$

where $\dot{U}^{(e)}$ and $\dot{U}_{m}^{(e)}$ stand for the total energy rate and the energy rate due to membrane effects only.

Clearly, under membrane conditions the value of $\dot{U}_{m}^{(e)}$ will be approximately equal to that of $\dot{U}^{(e)}$. This simple fact allows one to define the following scheme for choosing a membrane or bending formulation for the element:

1. At the onset of the deformation process the bending formulation is used for all elements in the sheet (Figure 2(a)).
2. Once the velocity solution has been obtained for each new deforming configuration, the following energy ratio parameter is computed for each element,

$$\xi^{(e)} = \frac{\dot{U}_{m}^{(e)}}{\dot{U}^{(e)}} \tag{31}$$

3. If $\xi^{(e)} < \xi_0$, where ξ_0 is a prescribed value close to unity, the effect of bending is assumed to be significant and the full element stiffness matrix of (24) is retained.
4. If $\xi^{(e)} > \xi_0$ the element is assumed to work under membrane conditions. This implies the following operations:

   4.1. A new stiffness matrix is computed for the element as

$$\mathbf{K}^{(e)} = \mathbf{K}_{m}^{(e)} \tag{32}$$

   where $\mathbf{K}_{m}$ contains the contribution of the membrane terms to the stiffness matrix.

   4.2. The 'transition' nodes shared by a patch of different elements working under bending and membrane conditions *retain the rotational degrees of freedom*. However, these contribute to the stiffness matrix of the bending elements only (Figure 2(b)). Examples of this combination of membrane and bending behaviour are very common in framed structures with internal pin-joints (Figure 3).

Axisymmetric Problems *3D problems*

a) Bending elements

$\mathbf{a}_i = [u_i, \omega_i, \theta_i]^T, \quad i = 1,2$ $\mathbf{a}_i = [u_i, v_i, \omega_i, \theta_{x_i}, \theta_{y_i}, \theta_{z_i}]^T, \quad i = 1,3$

b) Transition bending/membrane elements

$\mathbf{a}_1 = [u_1, v_1]^T$ $\mathbf{a}_1 = [u_1, v_1, \omega_1]^T$

$\mathbf{a}_2 = [u_2, \omega_2, \theta_2]^T$ $\mathbf{a}_i = [u_i, v_i, \omega_i, \theta_{x_i}, \theta_{y_i}, \theta_{z_i}]^T, \quad i = 2,3$

c) Membrane elements

$\mathbf{a}_i = [u_i, v_i]^T, \quad i = 1,2$ $\mathbf{a}_i = [u_i, v_i, \omega_i]^T, \quad i = 1,3$

Figure 2. Nodal variables for bending (b), membrane (m) and transition bending/membrane elements for axisymmetric and 3D sheet forming analysis

4.3. If *all* elements surrounding a node work under membrane conditions, the rotational degrees of freedom of the node can be eliminated (Figure 2(c)). This can be simply accomplished in practice by deleting the rows and columns corresponding to the nodal rotations in the element stiffness matrix.

Figures 4 and 5 show schematic examples of the different situations described above for 2D axisymmetric and 3D sheet forming processes.

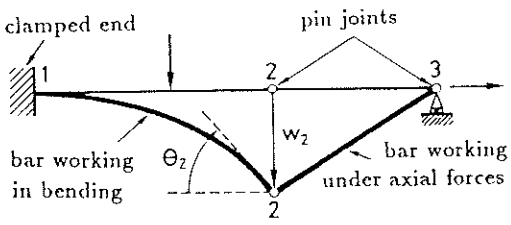

Effective displacement variables of node 2: ω_2, θ_2

Figure 3. Beam combining bending and axial elements

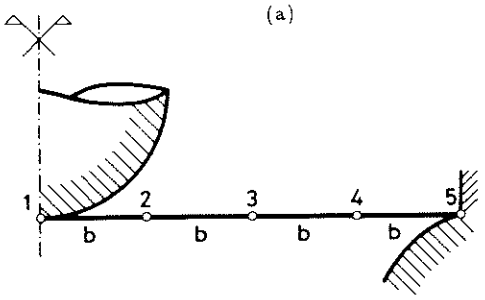

Degrees of freedom:

$$\mathbf{a}_i = [u_i, \omega_i, \theta_i]^T, \quad i = 1, \cdots, 5$$

Full $\mathbf{K}^{(e)}$ for all elements

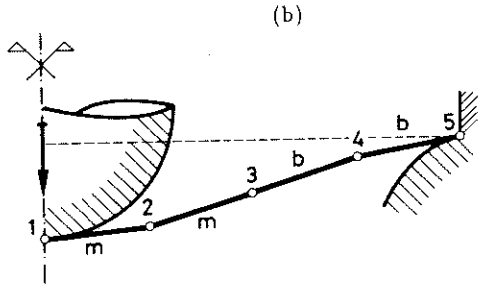

Degrees of freedom:

$$\mathbf{a}_i = [u_i, \omega_i]^T, \quad i = 1, 2$$
$$\mathbf{a}_i = [u_i, \omega_i, \theta_i]^T, \quad i = 3, 4, 5$$

Element	*Stiffness matrix*
$1-2$	$\mathbf{K}_m^{(e)}$ eliminating rows and columns of θ_1 and θ_2
$2-3$	$\mathbf{K}_m^{(e)}$ eliminating the row and column of θ_2
$3-4$ and $4-5$	Full $\mathbf{K}^{(e)}$

Figure 4. Axisymmetric sheet forming problem using selectively bending (b) and membrane (m) elements

a)

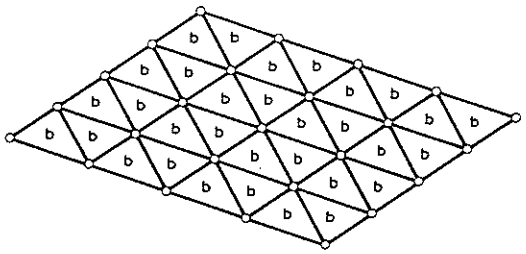

Full bending stiffness used in all elements

$$\mathbf{a_i} = [u_i, v_i, \omega_i, \theta_{x_i}, \theta_{y_i}, \theta_{z_i}]^T, \quad i = 1, n$$

b)

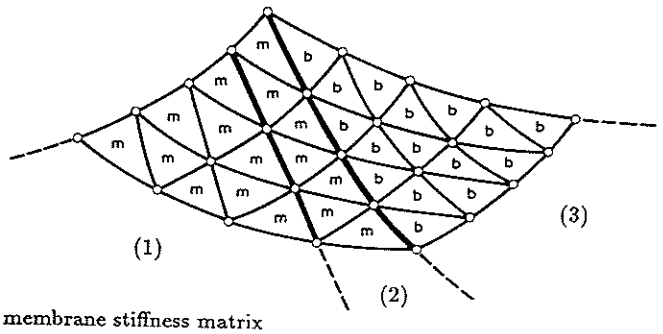

(1) Full membrane stiffness matrix

$$\mathbf{a}_i = [u_i, v_i, \omega_i]^T$$

(2) Transition bending/membrane elements

(3) Full bending stiffness matrix

$$\mathbf{a}_i = [u_i, v_i, \omega_i, \theta_{x_i}, \theta_{y_i}, \theta_{z_i}]^T$$

Full membrane region *Transition bending/membrane region*

$\mathbf{a}_i = [u_i, v_i, \omega_i]^T$
$\mathbf{K}_m^{(e)}$ for all elements

$\mathbf{a}_i = [u_i, v_i, \omega_i, \theta_{x_i}, \theta_{y_i}, \theta_{z_i}]^T$
$\mathbf{K}_m^{(e)}$ for membrane (m) elements
$\mathbf{K}^{(e)}$ for bending (b) elements

Figure 5. 3D sheet forming problem analysed using a selective bending (b) and membrane (m) finite element approach

Change from membrane to bending formulation

The contact of some parts of the sheet with sharp boundaries can lead to a drastic change from membrane to a bending situation. To detect these changes the value of the energy ratio ξ must be continuously checked throughout the whole deformation of the sheet. This implies keeping

a record of the nodal rotation rates at each deforming stage so that the bending energy rate can be adequately computed. The problem arises in membrane (or transition bending/membrane elements) in which the nodal rotation variables have been eliminated from all (or some) nodes. This difficulty can be overcome by computing first an *estimated* value of the element rotation from the element geometric changes between two consecutive deforming configurations. The corresponding nodal rotations are subsequently computed by a simple averaging of the rotations of all elements adjacent to the node.

This procedure is extremely simple for axisymmetric problems, as shown in Figure 6(a). For 3D problems the situation is somehow more complicated, particularly if large rotations are involved. However, assuming small rotations between two consecutive configurations, the problem is much simpler, since the components of the element rotations can be obtained from tensor transformations relating the known components of the normal vectors to the element at two consecutive configurations (Figure 6(b)).

a) *Axisymmetric problems*

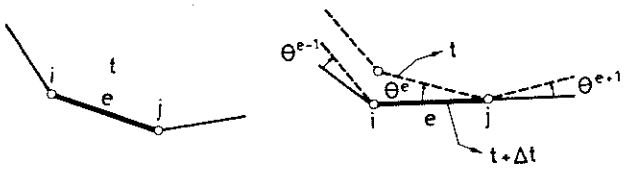

$$\theta_i = \frac{1}{2}(\theta^e + \theta^{e-1})$$

b) *3D problems*

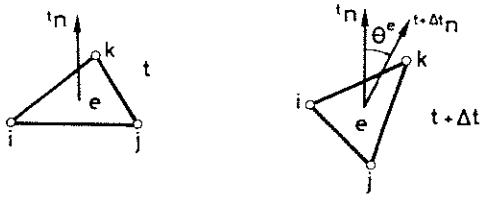

$$^{t+\Delta t}\mathbf{n} = \mathbf{T}\,{}^{t}\mathbf{n} \Rightarrow \theta_x^e, \theta_y^e, \theta_z^e$$

For small rotations:

$$\mathbf{T} = \begin{bmatrix} 1 & -\theta_z^e & \theta_y^e \\ \theta_z^e & 1 & -\theta_x^e \\ -\theta_y^e & \theta_x^e & 1 \end{bmatrix}$$

$$\theta^e = \left[(\theta_x^e)^2 + (\theta_y^e)^2 + (\theta_z^e)^2\right]^{\frac{1}{2}}$$

$$[\theta_{x_i}, \theta_{y_i}, \theta_{z_i}] = \frac{1}{n}\sum_{e=1}^{n}[\theta_x^e + \theta_y^e + \theta_z^e]\ ;\ i \in e$$

Figure 6. Computation of element and nodal rotations from geometrical changes

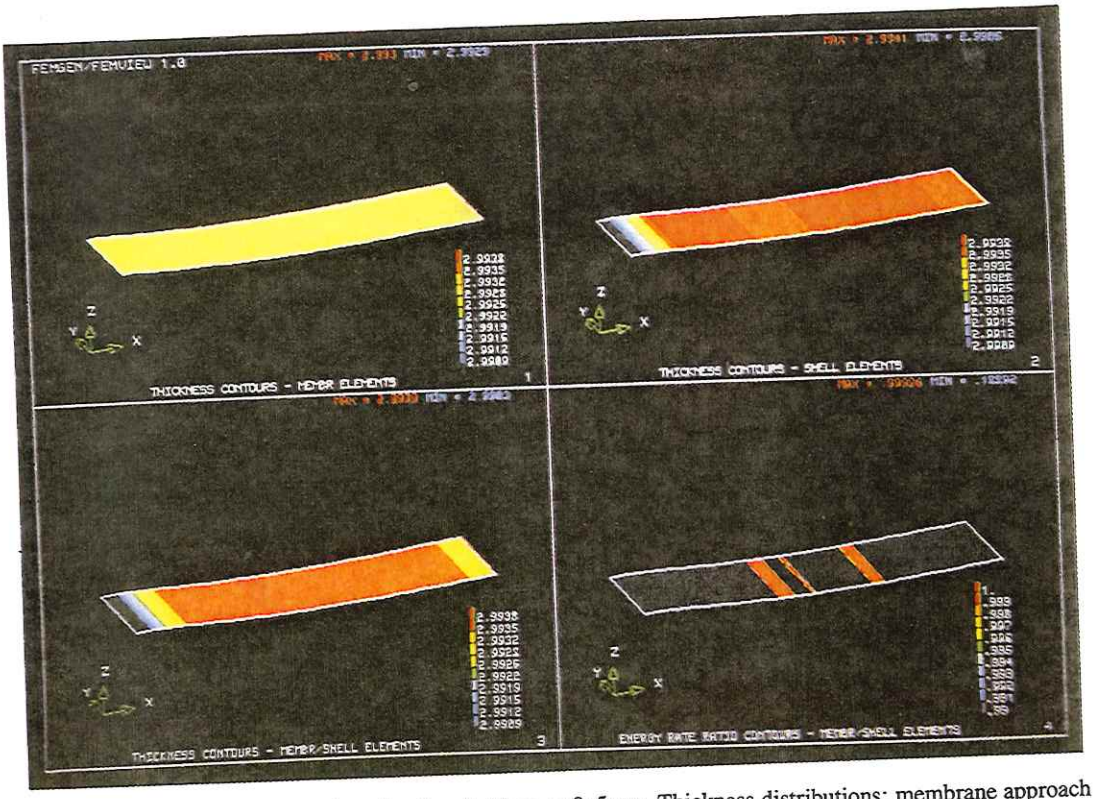

Plate 1. Superplastic forming of a strip. Step 1. Time = 8·5 sec. Thickness distributions: membrane approach (frame 1), bending approach (frame 2), selective bending/membrane approach (frame 3). Energy rate ratio distribution (frame 4)

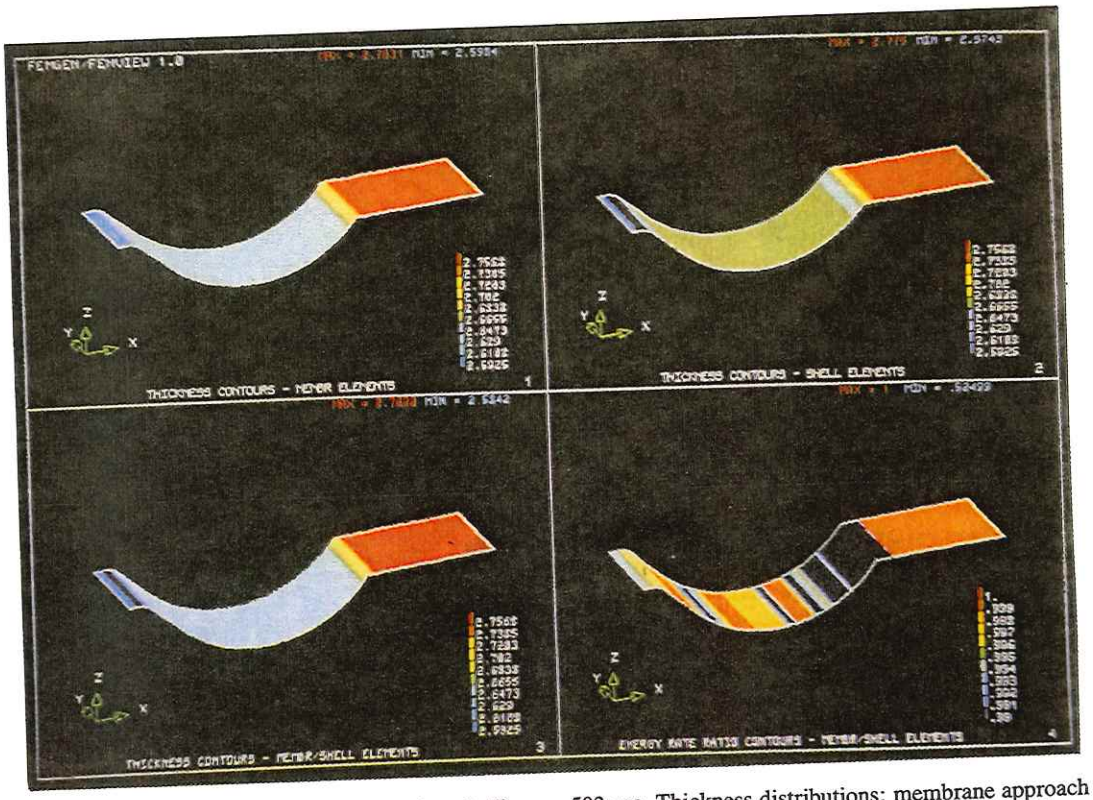

Plate 2. Superplastic forming of a strip. Step 3. Time = 503 sec. Thickness distributions: membrane approach (frame 1), bending approach (frame 2), selective bending/membrane approach (frame 3). Energy rate ratio distribution (frame 4)

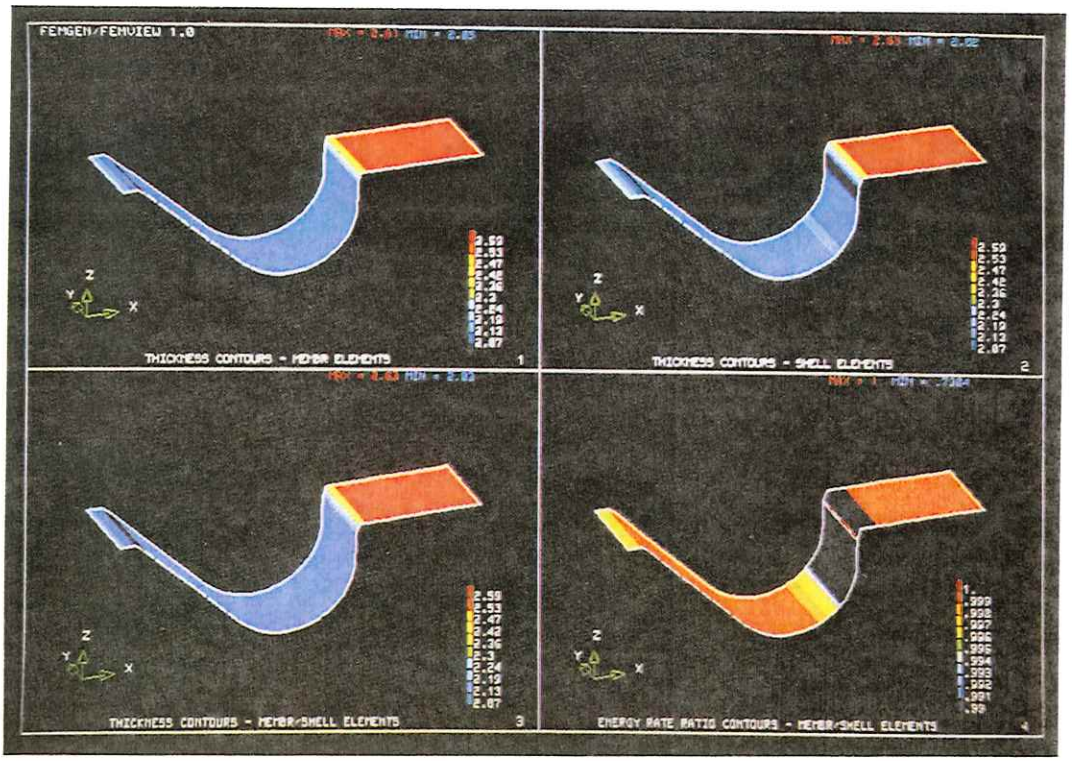

Plate 3. Superplastic forming of a strip. Step 5. Time = 1500 sec. Thickness distributions: membrane approach (frame 1), bending approach (frame 2), selective bending/membrane approach (frame 3). Energy rate ratio distribution (frame 4)

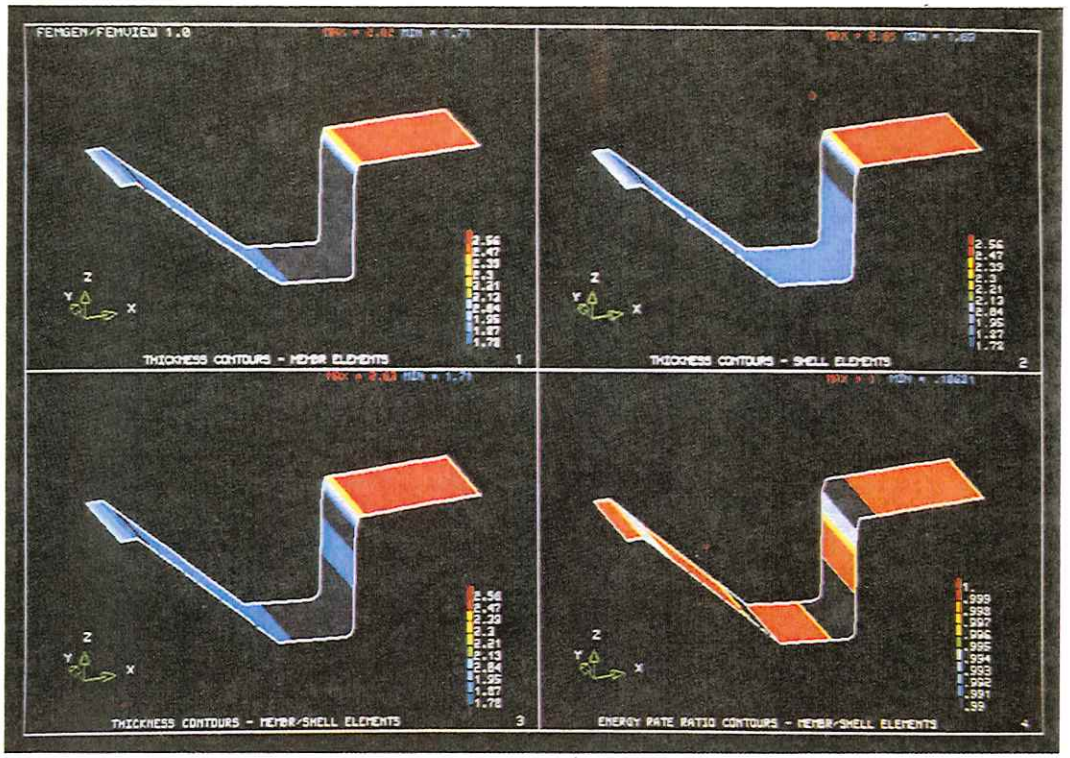

Plate 4. Superplastic forming of a strip. Step 7. Time = 3000 sec. Thickness distributions: membrane approach (frame 1), bending approach (frame 2), selective bending/membrane approach (frame 3). Energy rate ratio distribution (frame 4)

EXAMPLES

Example 1. Benchmark test for hemispherical punch stretching

This example corresponds to a benchmark test for numerical simulation of sheet metal forming processes, recently proposed by Wagoner *et al.*[17] The geometry of the sheet, punch and die is shown in Figure 7. The sheet material has been assumed to be rigid plastic with a strain hardening law given by

$$\bar{\sigma} = 589(10^{-4} + \bar{\varepsilon})^{0.216} \text{ MPa}$$

No porosity effects have been considered. Fourteen axisymmetric linear elements have been used in the analysis following the mesh spacing as suggested by Wagoner *et al.*[17] Contact between sheet and tools has been treated with a standard penalty formulation and friction effects have been modelled with a local non-linear Coulomb law.[12,14,18]

Figures 8(a) and (b) show the radial and hoop strain distributions obtained using a membrane and a full bending formulation for two friction coefficients of 0·0 and 0·3, respectively. It can be seen that the strain distributions for both formulations are almost identical, with the exception of some small discrepancies near the edge and the pole. This shows that a membrane formulation could be successfully used throughout the analysis.

This appreciation is confirmed by the curves of Figure 9 showing the energy rates ratio of (31), clearly indicating that the membrane energy dominates the solution along the whole deformation process. Also Figure 9 shows the above mentioned edge effect, which results in the need of using a full bending formulation in that zone.

This example has also been successfully analysed using the selective membrane/bending approach. Numerical results obtained in this case coincide exactly with those shown on Figure 8 for the bending formulation, as expected.

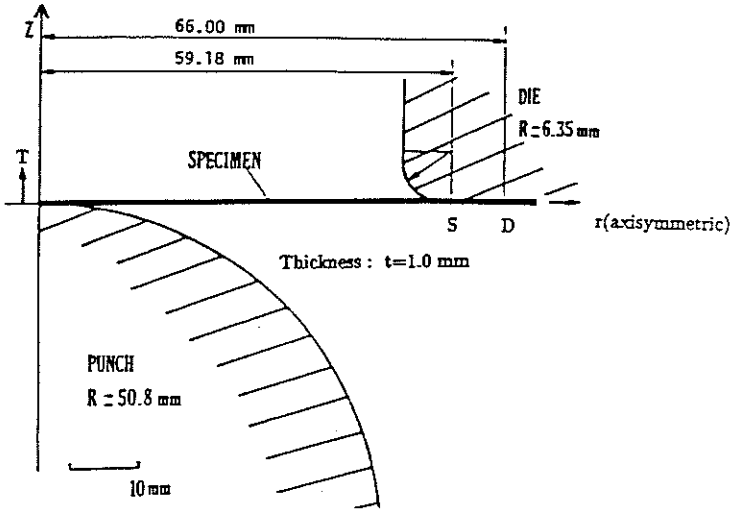

Figure 7. Geometry of the sheet and the tools for the Hemispherical Punch Stretching (HPS) benchmark test (Wagoner *et al.* 1988)

Example 2. Superplastic forming of a thin sheet under plane strain conditions

Figure 10 shows the geometry of the tool. Plane strain conditions have been assumed in the analysis. This simply implies neglecting circumferential effects in the axisymmetric shell formulation. Fourty-nine two node one dimensional elements have been used in the analysis. The material constitutive parameters are $k = 1200$ MPa sec^m and $m = 0{\cdot}6$. Contact between sheet and tool has been treated with a standard penalty formulation and full slipping condition (zero friction) at the contact regions has been assumed. A limit value for the energy ratio of $\xi_0 = 0{\cdot}99$ to define the change from bending to membrane condition has been chosen.

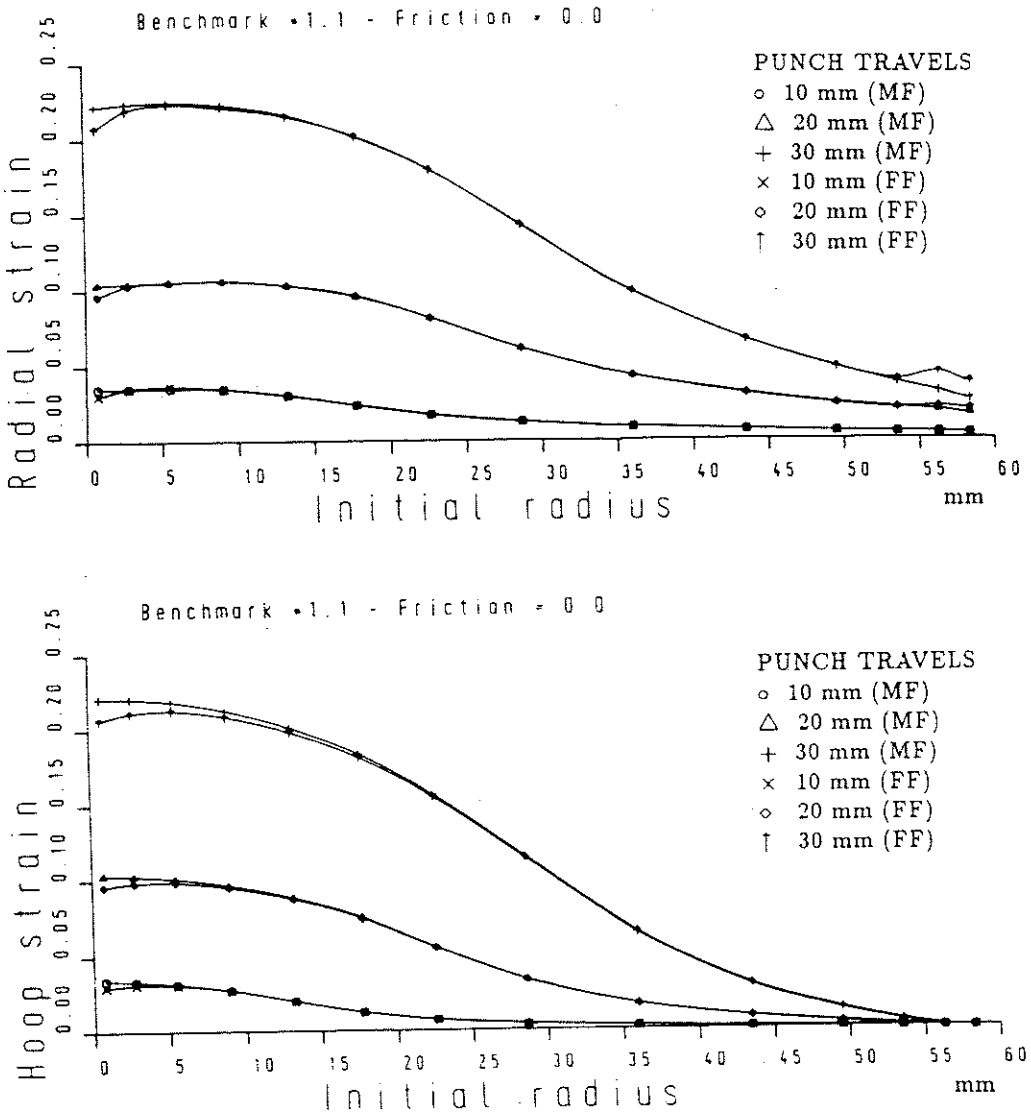

Figure 8(a). HPS benchmark test. Comparison between membrane (MF) and bending (FF) formulation. Radial and hoop strains for a friction coefficient of 0·0

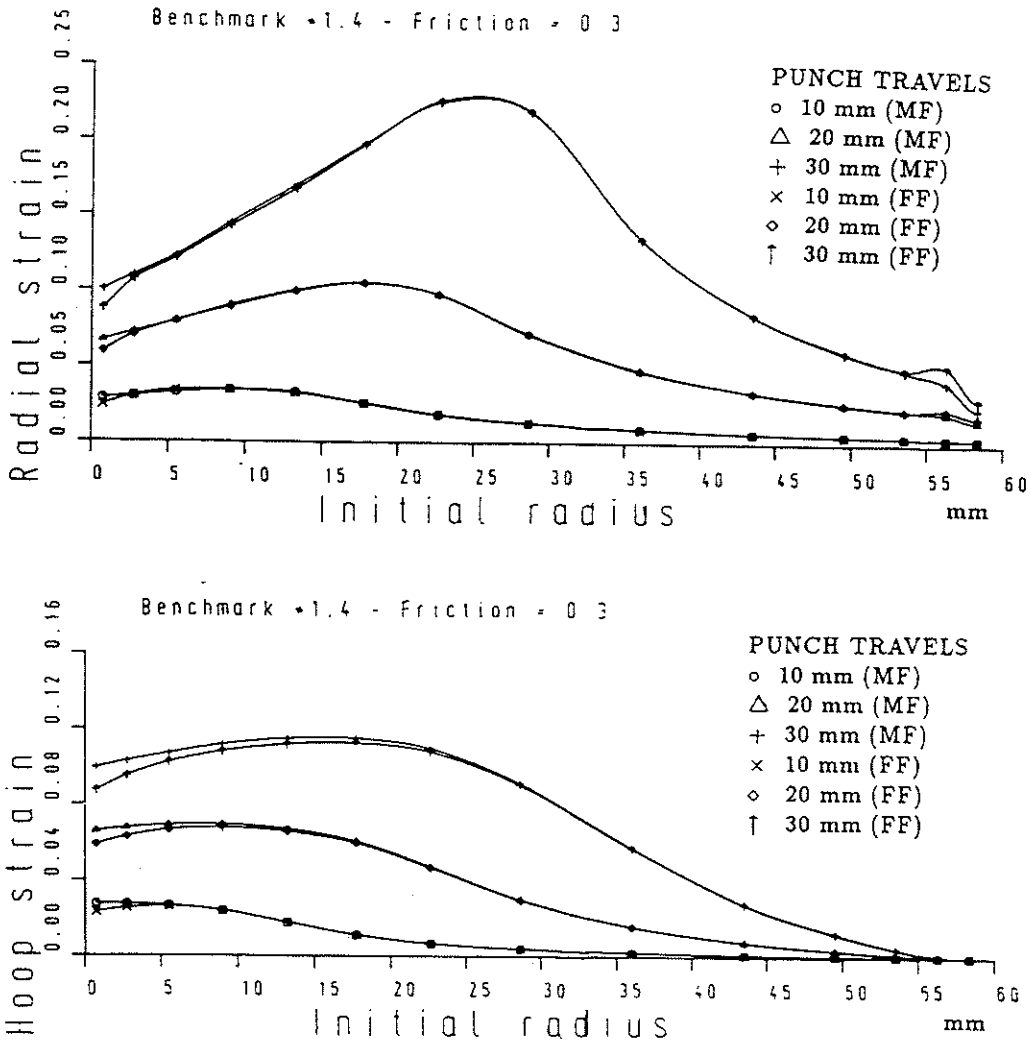

Figure 8(b). HPS benchmark test. Comparison between membrane (MF) and bending (FF) formulation. Radial and hoop strains for a friction coefficient of 0·3

Plates 1–4 show the thickness distribution at different deformation stages using membrane (frame 1), bending (frame 2) and selective bending–membrane (frame 3) formulations. Also the distribution of the energy rate ratio ξ at each deforming stage is shown in each plate (frame 4). The following points emerge from these plates.

(i) The values of the energy rate ratio ξ over the sheet at the onset of deformation are at many points below the limit value $\xi_0 = 0{\cdot}99$, thus indicating a global influence of bending in the early deformation stage (Plate 1). Bending elements are used in this case throughout most of the sheet, as clearly shown in Plate 1 (frame 4). (Bending and membrane elements are represented by dark blue and red zones, respectively.)

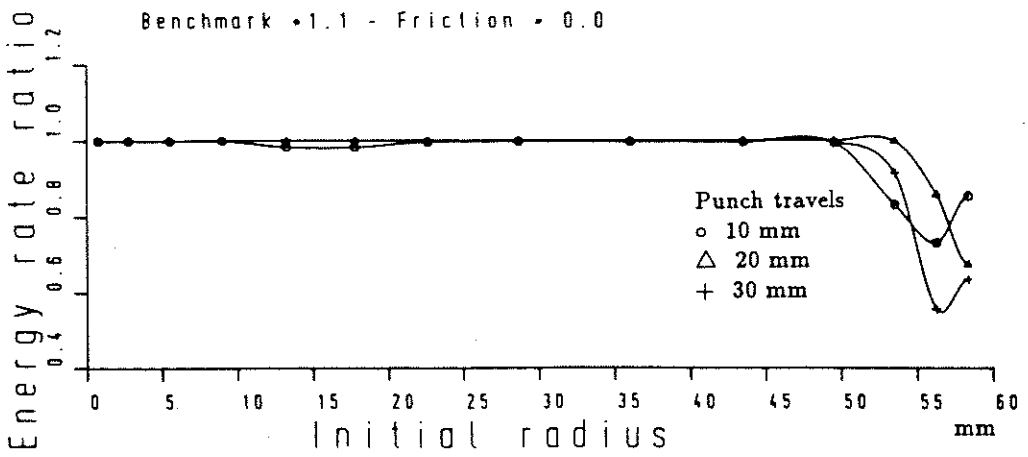

Figure 9. HPS benchmark test. Energy rate ratio at different punch travels

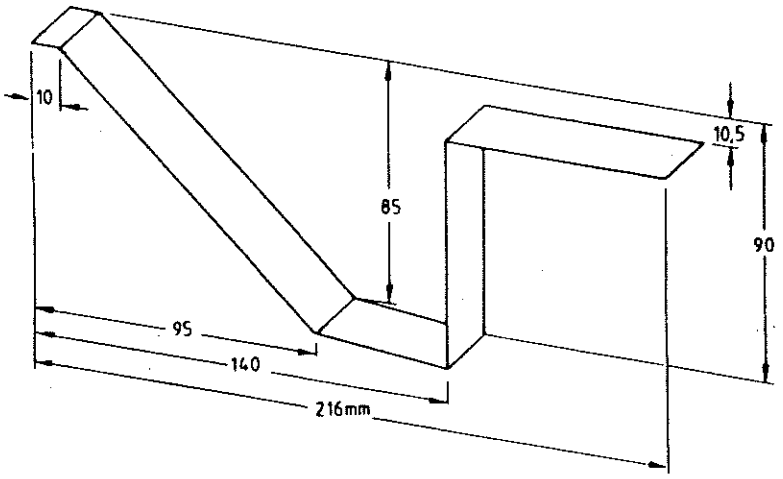

Figure 10. Superplastic forming (SPF) of a plane strip. Geometry of the forming tool

(ii) As deformation progresses the condition $\xi > \xi_0$ is satisfied in many parts of the sheet and membrane elements can be used in these zones (red areas in Plates 2–4, frame 4). Note that for well developed stages membrane theory can be used in $\simeq 80$ per cent of the mesh, thus introducing considerable economies in the solution process. An exception to this rule are the sharp corners where the low values of the energy rate ratio indicate the need of bending elements in those localized regions. It is also interesting to note that some elements near the bottom corners change from membrane to bending behaviour as contact with the tool progresses in that area.

(iii) Numerical results obtained for the thickness distribution with the selective bending/membrane formulation agree very well with those obtained with the full bending approach for all deforming stages.

CONCLUDING REMARKS

In this paper a selective bending/membrane viscous voided shell formulation for sheet metal forming problems has been presented. The preliminary results obtained for the simple axisymmetric cases studied show the potential of this approach for an effective and economical analysis of 3D real cases using complex punches and dies.

ACKNOWLEDGEMENTS

The authors are grateful for the financial support provided for this research by the European Economic Commission through BRITE contract No. RI–1B–0240–C (EL). Also the support of the Comisión de Investigación Científica y Técnica (CICYT) of the Ministerio de Educación y Ciencia of Spain through contract No. PB87–0603 is fully acknowledged. C. Agelet de Saracibar was also supported by a Fellowship from the Comissió Interdepartamental de Recerca i Innovació Tecnològica (CIRIT) of the Generalitat de Catalunya. This support is also gratefully acknowledged.

REFERENCES

1. O. C. Zienkiewicz, J. Bauer, K. Morgan and E. Oñate, 'A simple and efficient shell element for axisymmetric shells', *Int. j. numer. methods eng.*, **11**, 1545–1559 (1977).
2. O. C. Zienkiewicz, P. C. Jain and E. Oñate, 'Flow of solids during forming and extrusion. Some aspects of numerical solutions', *Int. J. Solids Struct.*, **14**, 15–38 (1978).
3. O. C. Zienkiewicz and P. N. Godbole, 'Flow of plastic and viscoplastic solids with special reference to extrusion and forming processes', *Int. j. numer. methods eng.*, **8**, 3–16 (1979).
4. O. C. Zienkiewicz, E. Oñate and J. C. Heinrich, 'A general formulation for coupled thermal flow of metals using finite elements', *Int. j. numer. methods eng.*, **17**, 1497–1514 (1981).
5. E. Oñate and O. C. Zienkiewicz, 'A viscous shell formulation for the analysis of thin sheet metal forming', *Int. J. Mech. Sci.*, **25**, 305–335 (1983).
6. J. F. T. Pittman, O. C. Zienkiewicz, R. D. Wood and J. M. Alexander (eds.), *Numerical Analysis of Forming Processes*, Wiley, New York, 1984.
7. E. Oñate, M. Kleiber and C. Agelet de Saracibar, 'Plastic and viscoplastic flow of void containing metals: Applications to axisymmetric sheet forming problems', *Int. j. numer. methods eng.*, **25**, 225–251 (1988).
8. O. C. Zienkiewicz, *The Finite Element Method*, McGraw-Hill, London, 1977.
9. A. L. Gurson, 'Continuum theory of ductile rupture by void nucleation and growth. I. Yield criteria and flow rules for porous ductile media', *J. Eng. Mater. Tech.*, **99**, 2–15 (1977).
10. E. Oñate and C. Agelet de Saracibar, 'Finite element analysis of sheet metal forming problems using a viscous voided shell formulation', in J. L. Chenot and E. Oñate (eds.), *Modelling of Metal Forming Processes*, Kluwer Academic Publishers, Dordrecht, 1988.
11. C. Agelet de Saracibar and E. Oñate, 'Plasticity models for porous metals', in D. R. J. Owen *et al.* (eds.), *Computational Plasticity: Models, Software and Applications*, Pineridge Press, Swansea, U.K., 1989.
12. E. Oñate and C. Agelet de Saracibar, 'Numerical modelling of sheet metal forming problems', in P. Hartley *et al.* (eds.), *Numerical Modelling of Material Deformation Processes: Research, Development and Applications*, Springer-Verlag, Berlin, to be published.
13. M. Kleiber, 'Numerical study on necking type bifurcations in void containing elastic plastic material', *Int. J. Solid Struct.*, **20**, 191–210 (1984).
14. J. B. Dalin and E. Oñate, 'An automatic algorithm for contact problems: Application to sheet metal forming', in E. G. Thompson *et al.* (eds.), *Numerical Methods in Industrial Forming Processes*, A.A. Balkema, Rotterdam, 1989.
15. E. Oñate, C. Agelet de Saracibar and J. B. Dalin, 'Finite element analysis of sheet metal forming problems using a selective voided shell membrane formulation', in E. G. Thompson *et al.* (eds.), *Numerical Methods in Industrial Forming Processes*, A.A. Balkema, Rotterdam, 1989.
16. C. Agelet de Saracibar and E. Oñate, 'Finite element analysis of sheet metal forming problems using a selective bending/membrane formulation', *Proc. 3rd Int. Conf. on Technology of Plasticity*, Kyoto, Japan, July 1–6, 1990, to appear.
17. R. H. Wagoner, E. Nakamachi and J. K. Lee, 'A benchmark test for sheet metal forming analysis', Ohio State University (to be published 1990).
18. J. T. Oden and E. B. Pires, 'Nonlocal and nonlinear friction laws and variational principles for contact problems in elasticity', *J. Appl. Mech. ASME*, **50**, 67–76 (1983).